



Effects of Vacuum Plasma Spray Processing Parameters on Splat Morphology

G. Montavon, S. Sampath, C.C. Berndt, H. Herman, and C. Coddet

Several statistical tools (i.e., Gaussian and Weibull distribution analyses, the t-test, and analysis of the variance) were used to examine relationships between vacuum plasma spray processing parameters and the morphology of flattened particles (splats) on a smooth, polished substrate. Astroloy, a nickel-base powder, was vacuum plasma sprayed onto polished copper substrates under various processing conditions. Different flattened particle shape factors, including equivalent diameter, elongation factor, and degree of splashing, were determined using image analysis. The spray parameters (i.e., current intensity, chamber pressure, argon mass flow rate, etc.) strongly influenced splat formation and morphology and thus deposit microstructure and properties.

1. Introduction

ALTHOUGH commonly used by industry, direct-current plasma spraying—particularly vacuum plasma spraying (VPS)—has developed through trial-and-error empirical approaches. This is essentially because VPS is relatively complex; more than 50 interrelated parameters that influence the process have been identified (Ref 1). For example, the effect of coating microstructure on mechanical properties is not well defined, and the relationships between controllable spray parameters and coating microstructure are understood to only a limited degree.

Vardelle et al. (Ref 2) investigated the influence of several important processing parameters on the velocity and temperature of particles within the plasma plume. A compromise apparently exists between particle temperature and velocity. For example, increased jet constriction induces increased jet velocity (and thus increased particle velocity), but simultaneously induces decreased plume temperature by enhancing the engulfment of the surrounding atmosphere. Therefore, the optimum condition is based on the desired flattening behavior of the individual droplet (particle).

The manner in which the deposit properties are linked to the deposit microstructure is controlled by the flattening of the impinging particles onto the substrate or previously deposited layers (Ref 3). The influence of spray parameters on the morphology of flattened particles has been investigated (Ref 4-6). Other studies have considered the influence of surface roughness (Ref 7), the effects of surface orientation (Ref 8, 9), and the effect of coating thickness (Ref 10). Surface roughness strongly modifies particle flattening, whereas an off-normal substrate orientation influences splat morphology. However, no clear quantitative relationships have been demonstrated between these variables and deposit properties. Additionally, in the

Keywords: flattened particle, image analysis, processing parameter, statistical analysis, vacuum plasma spraying

G. Montavon and C. Coddet, Laboratoire d'Etudes et de Recherches sur les Matériaux et les Propriétés de Surface, Institut Polytechnique de Sévenans, Belfort, France; S. Sampath, C.C. Berndt, and H. Herman, Thermal Spray Laboratory, Department of Materials Science and Engineering, State University of New York at Stony Brook, Stony Brook, NY 11794-2275, USA

case of VPS, the influence of chamber pressure and the effects of the elongated plasma plume on splat formation are not unambiguously established.

The present work examines the influence of various spray parameters, including gas mixture, chamber pressure, and current intensity, on the characteristics of individual flattened particles sprayed onto polished substrates. Statistical tools such as

Table 1 Chemical composition of Astroloy

Element	Weight percent	Element	Parts per million
Nickel	bal	Boron	2000
Cobalt	18.80	Carbon	2000
Chromium	14.90	Silicon	2000
Molybdenum	4.99	Oxygen	85
Aluminum	3.99	Nitrogen	29
Titanium	3.55	Sulfur	5
Iron	0.11		
Zirconium	0.04		

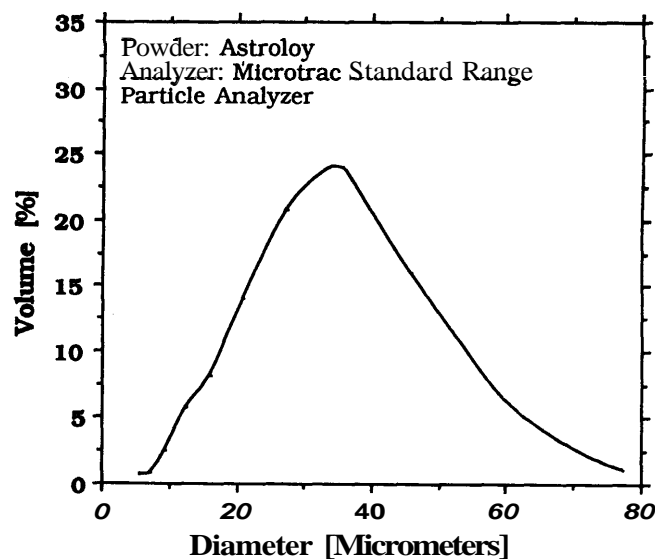


Fig. 1 Grain size distribution of Astroloy

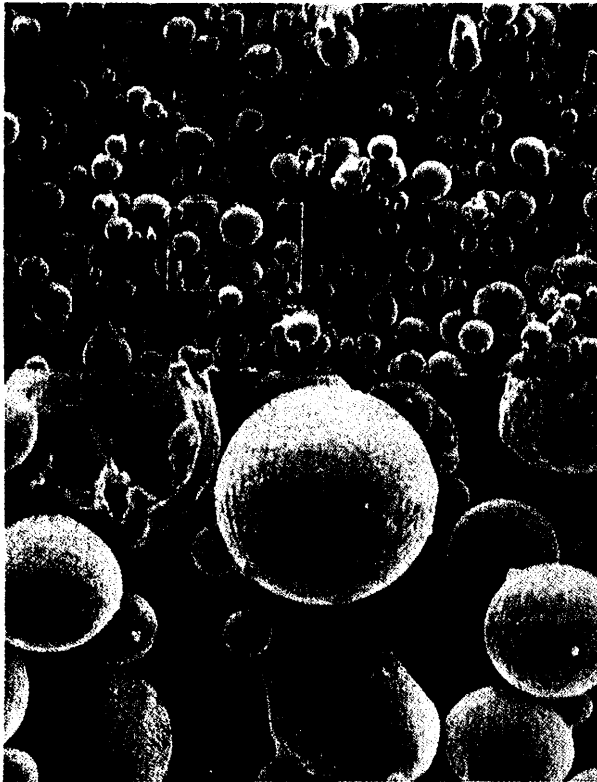


Fig. 2 Scanning electron micrograph of the Astroloy powder particles.

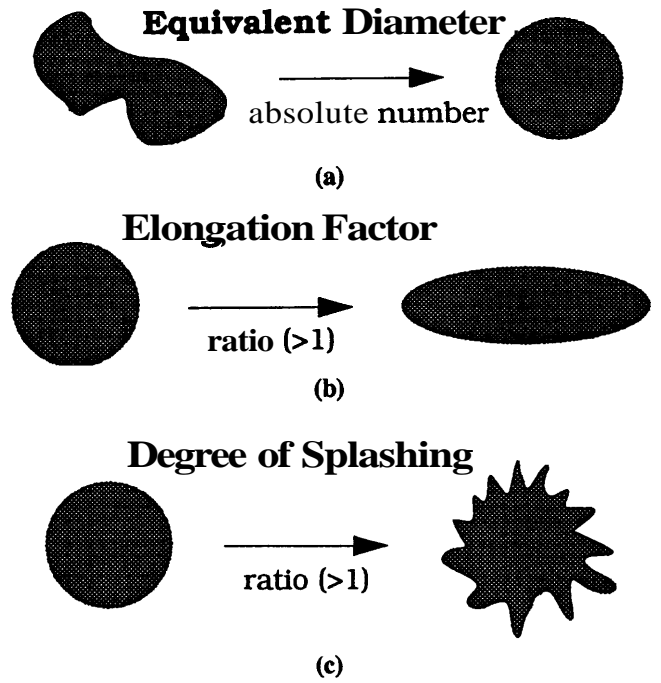


Fig. 3 Equivalent diameter, elongation factor, and degree of splashing of a splat. (a) is an absolute number whereas (b) and (c) are ratios where a number greater than unity represents an increase in tendency to elongate or splash, respectively.

Table 2 Taguchi L8 (2^7) alias structure (a)

Test	A	B	C	D	E	F	G
TA01	-	-	-	-	-	-	-
TAM	+	-	+	-	+	-	+
TA03	-	+	+	-	-	+	+
TAW	+	+	-	+	+	+	-
TA05	-	-	-	+	+	+	+
TA06	+	-	+	+	-	+	-
TA07	-	+	+	+	+	-	-
TA08	+	+	-	+	-	-	+

(a) The L8 designation refers to a two-level orthogonal matrix constituted by eight tests and extrapolated from a 2^7 factorial design. The + and - signs represent the upper and lower levels of the design, respectively.

Table 3 Spray parameters for VPS deposition

Test	P1	P2	P3	Spray parameter (a)			
				P4	P5	P6	P7
TA01	650	60	60	6	300	4	3
TA02	650	60	40	10	240	2.8	3
TA03	650	120	60	6	300	2.8	3
TAW	650	120	60	10	240	4	3
TA05	720	60	60	6	240	2.8	3
TA06	720	60	60	10	300	4	3
TA07	720	120	40	6	240	4	3
TA08	720	120	40	10	300	2.8	3
TA09(b)	700	60	50	8	270	3.4	3

Note: The relative gun/substrate velocity was kept constant and equal to 1 m/min during the entire set of Taguchi experiments. (a) P1, current intensity (A); P2, chamber pressure (mbar); P3, argon volume flow rate (L/min); P4, hydrogen volume flow rate (Umin); P5, spray distance (mm); P6, carrier gas (argon) volume flow rate (L/min); P7, powder feed rate (g/min).

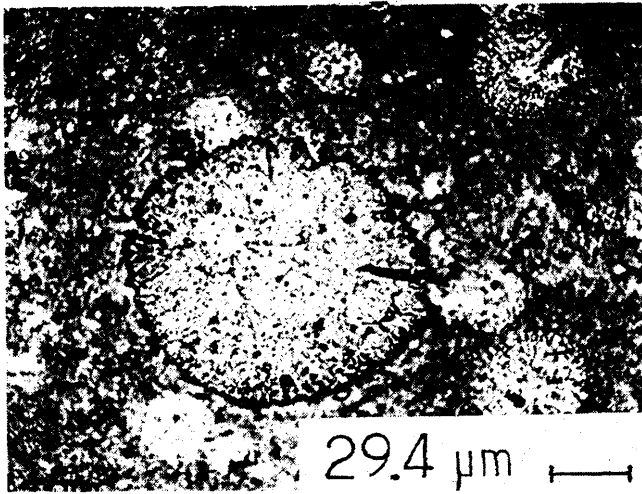


Fig. 4 Typical splat morphology (TA06 spray parameter set)

Gaussian analysis, Weibull distribution analysis, the t-test, and analysis of the variance are implemented.

2. Experiments

2.1 Material Characterization

The feedstock was Astroloy, a nickel-base alloy (Table 1), with a particle size distribution as shown in Fig. 1. The particle morphology (Fig. 2) was characterized as spherical, a shape typically obtained from the gas atomization process.

2.3 Spray Conditions

The substrates were ground and polished to determine the characteristics of individual flattened particles. The polishing consisted of grinding with 600 grit SiC paper, followed by diamond slurry polishing using, in sequence, 5, 1, and 0.1 μm diamond grit. After polishing, the substrates exhibited surface roughnesses ranging from 0.1 to 0.3 μm .

The powder was vacuum plasma sprayed at chamber pressures of 60 and 120 mbar in an inert residual atmosphere of argon using a Plasma-Technik (Plasma-Technik AG, Wohlen, Switzerland) F4-VB gun with a divergent nozzle. One pass at 1 m/min velocity was performed in front of each sample.

The influence of various spray parameters can be studied using a number of statistical design of experiment strategies. The Taguchi method permits definition of the influences of the processing parameters and their relative importance (Ref 11). The "analysis of the variance" (ANOVA) method allows precise determination of the influence of each parameter over the measured results (Ref 12) by determining the ratio of the calculated Fisher number to the listed Fisher number. The Fisher number, defined as the ratio of the parameter variance to the residue variance, outlines the importance of a given parameter compared to the effect of the residue. In this study, a Taguchi L8 (2^7) experimental design without repetition was used to build the different experimental sets (Tables 2 and 3). In such a case, the sum of the

two smallest average values is taken as a residue (data pooling) (Ref 12). This residue is used to calculate the Fisher numbers; the effects of the resulting test parameters are considered negligible (Ref 13).

2.3 Image Analysis

The splat characteristics were measured using optical microscopy and image analysis. Various shape factors were considered (Ref 14): the equivalent diameter (ED), defined as the diameter of a circle with the same area as the selected feature; the elongation factor (EF), defining the noncircular nature of the selected feature (unity being a perfect circle); and the degree of splashing (DS), indicating the importance of peripheral material projections at the impact (unity resulting from the absence of such projections). The mathematical relationships of these shape factors are

$$ED = \left(\frac{4A}{\pi} \right)^{1/2} \quad (\text{Eq 1})$$

$$EF = \left(\frac{\pi}{4} \right) \left(\frac{L^2}{A} \right) \quad (\text{Eq 2})$$

$$DS = \left(\frac{1}{4\pi} \right) \left(\frac{P^2}{A} \right) \quad (\text{Eq 3})$$

where A is the area of the selected feature (mm^2), L is the longest dimension (mm), and P is the perimeter (mm) (Fig. 3).

Each measurement series of 50 readings was randomly located. The resulting data were adjusted by subtracting the two largest and the two smallest data points to discriminate against atypical values. The presented results refer to the adjusted data.

3. Statistical Analysis

Several statistical analyses were performed on the collected data. The data scatter was determined using the mean value, μ , and the standard deviation, σ , of the Gaussian distribution (Ref 15). The variability within the distributions was estimated by calculating the Weibull parameters—that is, Weibull modulus, m, and characteristic value, x_0 (Ref 16), which, respectively, reflect the data scatter and the 63.2% percentile of the cumulative density. Determination of these parameters was accomplished by the curve-fitting method (Ref 17-20).

The data were discriminated using the t-test (Ref 21). This statistical procedure compares the hypothesis that the means of data sets are, or are not, identical—assuming that the sample populations of the data sets belong to Gaussian distributions.

4. Results and Discussion

4.1 Optical Observation

Figure 4 shows the morphology of splats on a smooth surface. The "pancake" shape indicates a homogeneous molten state of the particle before the impact (Ref 5) and, very likely, a

Table 4 Flattened particle characteristics

Test	ED, mm			EF			DS		
	μ	σ	σ/μ	μ	σ	σ/μ	μ	σ	σ/μ
TA01	0.107	0.033	0.308	1.35	0.10	0.07	1.77	0.39	0.22
TA02	0.096	0.039	0.406	1.24	0.07	0.05	1.35	0.17	0.12
TA03	0.096	0.032	0.333	1.38	0.14	0.10	1.83	0.39	0.21
TA04	0.100	0.030	0.300	1.43	0.16	0.11	2.09	0.47	0.22
TA05	0.094	0.031	0.330	1.32	0.13	0.10	1.59	0.39	0.24
TA06	0.088	0.032	0.363	1.45	0.13	0.09	2.03	0.38	0.19
TA07	0.078	0.023	0.294	1.34	0.12	0.09	1.65	0.37	0.22
TA08	0.087	0.027	0.310	1.39	0.11	0.08	1.93	0.34	0.17
TA09(a)	0.090	0.033	0.366	1.37	0.12	0.09	2.00	0.39	0.19

(a) Referencespray parameters(i.e., parameters used by the LERMPS-IPSe)

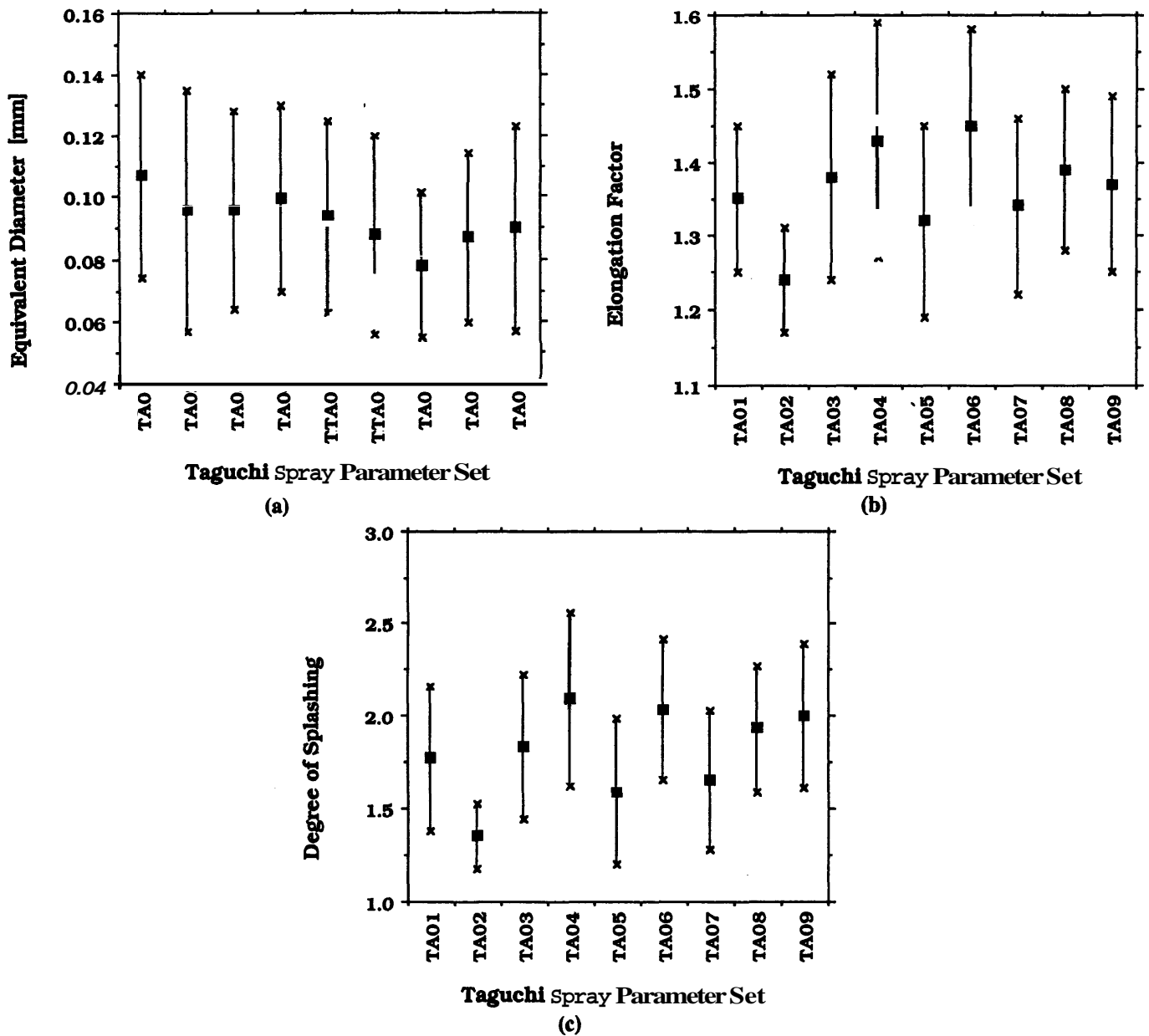


Fig. 5 Arithmetic average and standard deviation (represented by error bar) of the splat characteristics. (a) Equivalent diameter. (b) Elongation factor. (c) Degree of splashing

complete flattening of the particles prior to solidification (Ref 22).

4.2 Gaussian Analysis

The results of the Gaussian analyses are summarized in Table 4 and Fig. 5, where error bars indicate the standard deviation. The data indicate that the variations of the spray parameters in the examined range did not substantially modify the particle morphologies. This is not surprising, because the range of the parameters was relatively small and close to the reference parameters (i.e., parameters developed and commonly used at France's LERMPS-IPSC) in order to optimize the process.

The relationship between the degree of splashing and the equivalent diameter of particles can be outlined. For example, Fig. 6 displays this evolution for the TA02 and TA04 spray parameter sets, which are characterized by the two extreme values of the arithmetic average of the degree of splashing (1.35 and 2.09, respectively). A general trend is that smaller particles do not splash as much as larger ones. Moreover, this trend depends on the spraying parameters and is less pronounced for the TA02 spray parameter set, which is characterized by the highest ratio of hydrogen mass flow rate to argon mass flow rate (H_2/Ar) and the lowest chamber pressure of the Taguchi design. The physical explanation of such correlations is that the higher-momentum particles cannot dissipate energy sufficiently rapidly during impact against the substrate and that the solidification during the

splat process provides artificial protuberances that give rise to splashing.

The ANOVA method has been performed over these data to better understand the relative influence of each spray parameter. The spray parameters do not significantly affect the elongation factor and the degree of splashing in the examined range, but do affect the equivalent diameter. Table 5 summarizes the ANOVA

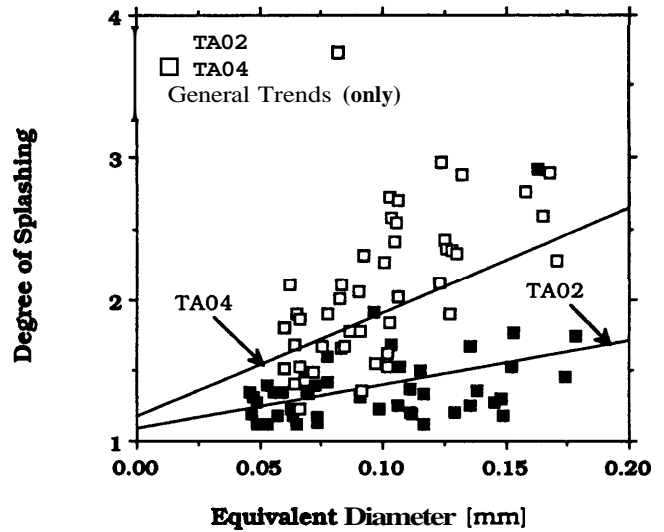


Fig. 6 General trend and evolution of the degree of splashing of splats versus their equivalent diameter (TA02 and TA04 data)

Table 5 ANOVA analysis of equivalent diameter results
Confidence level of 95%

Spray parameter(a)	Calculated Fisher number	Tabulated Fisher number	Effect	Rank
P1	Insignificant	6
P2	142	18.2	Significant	3
P3	224	18.2	Significant	2
P4	622	18.2	Significant	1
P5	2.2	18.2	Insignificant	4
P6	2.2	18.2	Insignificant	4
P7	Insignificant	6

Note: The tabulated Fisher number is equal to the degree of freedom of the data over the degree of freedom of the residue, taken as respectively equal to 7 and 2. If the calculated Fisher number is greater than the tabulated Fisher number, the effect of the parameter is considered to be significant and vice versa (a) See Table 3 for definition of spray parameters.

Table 6 Weibull analysis of equivalent diameter, elongation factor, and degree of splashing data

Test	ED			EF			DS	
	m	x_0	m	x_0	m	x_0		
TA01	3.6	0.118	15.0	1.39	5.1	1.92		
TA02	2.6	0.108	18.1	1.27	8.9	1.42		
TA03	3.4	0.107	10.4	1.45	5.2	1.99		
TA04	3.8	0.110	9.4	1.51	5.0	2.28		
TA05	3.4	0.105	11.0	1.38	4.6	1.74		
TA06	3.2	0.099	12.0	1.51	6.1	2.19		
TA07	3.5	0.088	12.5	1.39	5.2	1.79		
TA08	3.7	0.097	13.8	1.43	6.3	2.07		
TA09(a)	3.1	0.101	12.4	1.42	5.8	2.16		

(a) Reference spray parameters (i.e., parameters used by the LERMPS-IPSC)

results for these data at a confidence level of 95%. The influence has been ranked, from a general point of view, from the most influential (rank number 1) to the least (rank number 6). Three controllable spray parameters produce significant effects: hydrogen mass flow rate, argon mass flow rate, and chamber pressure. The first two parameters influence the velocity field in the plasma flame (Ref 23) and therefore the dwell time of the particles and their velocities at impact. They also influence the temperature field of the plasma flame (Ref 24) and hence the heat transfer between particles and the surrounding gases as well as the viscosity of the particles on impact.

4.3 Weibull Analysis

Weibull characteristics are listed in Table 6. The calculated Weibull moduli can be classified as low (between 2.6 and 3.8) for the distributions of equivalent diameter, indicating a large variability in the data. This is directly related to the particle size distribution of the powder. The Weibull moduli of the distributions of the elongation factor can be classified as relatively high (between 18.1 and 9.4), indicating a small variability in the data. It can be assumed that this narrow distribution is partly induced by the normal spray angle (e.g., 90°), which remained constant for the entire set of experiments.

The Weibull moduli of the distributions of the degree of splashing ranged from a maximum of 8.9 (TA02 spray parameter set) to a minimum of 5.0 (TA04 spray parameter set), indicating a moderate variability in the data. Weibull plot analyses performed over the data for the 25 smallest and 25 largest equivalent diameters established a clear relationship between these equivalent diameters and the corresponding degree of splashing. Table 7 summarizes the results relative to the Weibull analysis of TA02 and TA04 data. Deposited particles of high equivalent diameter tended to exhibit more splashing.

Table 7 Weibull analysis of degree of splashing data for the 25 smallest and 25 largest resulting equivalent diameters

Test	Smallest ED		Largest ED	
	m	x_0	m	x_0
TA02	19.6	1.25	11.1	1.55
TA04	8.8	1.80	8.2	2.62

Table 8 t-test comparison of particle characteristics

ED, EF, and DS indicate similarities (i.e., t value greater than 0.1) between the data

Test	TA01	TA02	TA03	TA04	TA05	TA06	TA07	TA08	TAW
TA01									
TA02			ED	ED	ED		EF		
TA03					ED				EF
TA04						EF DS			
TA05									
TA06								ED	ED
TA07									
TA08									ED
TA09(a)									

(a) Reference spray parameters (i.e., parameters used by the LERMPS-IPSe)

4.4 t-Test Analysis

The particle characteristics were compared using the t-test protocol. Table 8 presents the results. Gaussian analysis of equivalent diameter was confirmed by the results of the t-test, which indicated similarity between the data. The data sets showed significant variations in the elongation factor, indicating that the spread of an impinging particle on the substrate surface is a random phenomenon. In terms of degree of splashing, as discussed earlier the data sets showed a considerable variability with spray parameters.

The similarities between the mean values of the distributions of TA04 and TA06 data are interesting. They seem to indicate that the velocity/temperature pairs of the particles at the impact are similar, although the spray parameters are different; that is, decreasing the chamber pressure allows higher spraying distances.

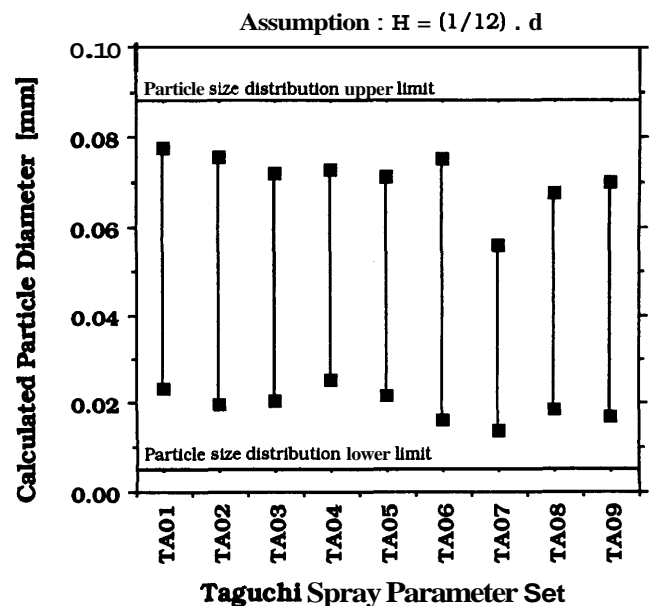


Fig. 7 Variations of the lower and upper limits of the calculated powder particle diameters leading to splat formation for the different Taguchi spray parameter sets



4.5 Geometric Relationships

Different relationships defining geometric links between the diameter of the impinging particle and the diameter and thickness of the resulting flattened particle have been theoretically and experimentally determined. Among these, the **Madejski** relationships (Ref 8) are expressed as:

$$D = (1.29d)(Re^{0.2}) \quad (\text{Eq 4})$$

$$H = \left(\frac{2}{3}\right) \left(\frac{d^3}{D^2}\right) \quad (\text{Eq 5})$$

where D and H , respectively, are the diameter and the thickness of the splat, and d and Re , respectively, are the diameter and the Reynolds number of the impinging particle.

Liu et al. (Ref 25) and **Kitaura** et al. (Ref 26) have linked the thickness of a splat with the diameter of the impinging particle. It appears that this thickness is in the range of one-tenth the diameter of the impinging particle.

By rearranging Eq 4 and 5, the diameters of impinging particles that could lead to the formation of splats were defined, assuming that (1) the **thickness/equivalent** diameter ratio remains constant and equal to one-twelfth, regardless of the equivalent diameter; (2) no partial vaporization of the particles occurs to influence splat formation; (3) the splats are considered to be perfectly cylindrical (**i.e.**, constant thickness); and (4) the degrees of flattening of the impinging particles are close, regardless of the initial diameter. The results were then compared with the particle size distribution of the powder. Figure 7 illustrates the evolution of the extreme values obtained (**e.g.**, smallest and largest diameters) for the different Taguchi spray parameter sets. The lower and upper limits of the particle size distribution of the powder—equal to 5 and 88 μm (0.005 and 0.088 mm), respectively—are also indicated.

It appears that only a fraction of the available particle sizes is used to form the splats, this fraction being related to the spray parameters. The smallest particles are probably vaporized in the plasma, the amount depending on plasma temperature and velocity. The largest particles can be partially or completely unmolten on impact against the substrate and hence rebound from the surface of the substrate, or their normal velocity can be lower than a critical velocity necessary to induce spreading.

Such a method can be easily implemented to optimize spray parameters for a given feedstock material. The results allow specifications to be defined, especially those relative to optimal particle size distribution, which may lead to minimal loss of powder.

5. Conclusion

Geometric characteristics of **Astroloy** splats on polished copper substrates were examined using optical microscopy with image analysis. The effects of several controllable spray parameters on the resulting particle shapes were investigated. These spray parameters influence velocity and temperature fields and therefore splat formation. Three primary spray parameters significantly affect the equivalent diameters (**i.e.**, flattening of the particles) of the splats: the chamber pressure and

the argon and hydrogen mass flow rates (parameters that influence the velocity and the temperature of a particle before impact). However, the elongation factor remains insensitive to these parameters. In every case, a "pancake" shape was observed, indicating a completely molten particle state at impact.

Results of different statistical analyses were combined to identify the main characteristics of flattened particles as a function of spray **parameters**. The t-test permitted estimation of the similarities between the data, indicating (1) a relative similarity between the equivalent diameters, regardless of the selected spray parameter set in the considered range; and (2) significant differences in the elongation factor and in the degree of splashing, the spread of an impinging particle being a random phenomenon.

Determination of the Weibull parameters allowed definition of the variability of the distributions as a function of the spray parameters, indicating low moduli for the equivalent diameters (and thus a high variability directly linked to particle size distribution) and high moduli for elongation factors and degrees of splashing. It appeared that the larger the size of the impinging particle, the higher the probability for the splashing phenomenon to occur.

The particle diameters that could lead to the formation of the measured splats were also determined, assuming a constant splat thickness equal to one-twelfth the diameter of the impinging particle. The splats result from a selected fraction of the particle size distribution. It was assumed that the smallest particles are vaporized in the plasma flame during flight and that the largest particles are partially unmolten and may rebound at the substrate surface or may have a velocity lower than a critical value necessary for spreading to occur.

Acknowledgments

This study was supported by the French government under Grant No. MRT 91A0381; by the French companies **Turboméca**, **Société Européenne** de Propulsion, and Sochata; and by the NSF **STRATMAN** initiative under Grant No. DDM9215846.

References

1. I.A. Fisher, Variables Influencing the Characteristics of Plasma-Sprayed Coatings, *Int. Metall. Rev.*, Vol 164 (No. 17), 1972, p 117-129
2. M. Vardelle, A. Vardelle, and P. Fauchais, Spray Parameters and Particle Behavior Relationships during Plasma Spraying, *J. Therm. Spray Technol.*, Vol 12 (No. 1), 1993, p 79-91
3. C. Moreau, M. Lamontagne, and P. Cielo, Temperature Evolution of Plasma-Sprayed Niobium Particles Impacting on a Substrate, *Thermal Spray Research and Applications*, T.F. Bernecki, Ed., ASM International, 1991, p 19-26
4. O.P. Solonenko, The Fundamental Thermophysical Problems of Plasma-Spraying, *Thermal Spray: International Advances in Coatings Technology*, C.C. Berndt, Ed., ASM International, 1992, p 787-792
5. J.M. Houben, Future Development in Thermal Spraying, *Proc. 2nd Natl. Conf. Thermal Spray* (Long Beach, CA), ASM International, 1985, p 1-12
6. M.P. Planche, O. Betoule, J.F. Coudert, A. Grimaud, M Vardelle, and P. Fauchais, Performance Characteristics of a Low Velocity Plasma Spray Torch, *Thermal Spray Coatings: Research, Design and Applica-*

- tions, C.C. Berndt and T.F. Bernecki, Ed., ASM International, 1993, p 81-87
7. S. **Fantassi**, M. Vardelle, A. Vardelle, and P. Fauchais. Influence of the Velocity of Plasma Sprayed Particles on the Splat Formation, Thermal Spray Coatings: Research, Design and Applications. C.C. Berndt and T.F. Bernecki, Ed., ASM International, 1993, p 1-6
 8. J. **Madejski**, Solidification of Droplets on a Cold Surface, *Int. J. Heat Mass Transfer*, Vol 19, 1976, p 1009-1013
 9. A. **Hasui**, S. **Kitahara**, and T. Fukushhna, On Relation between Properties of Coating and Spray Angle in Plasma Jet Spraying, *Trans. Natl. Res. Inst. Met.*, Vol 12 (No. 1), 1970, p 9-20
 10. C. Moreau, M. **Lamontagne**, and P. Cielo, Influence of the Coating Thickness on the Cooling Rate of Plasma-Sprayed Particles Impinging on a Substrate, Thermal Spray Coatings: Properties, Processes and Applications, T.F. Bernecki, Ed., ASM International, 1992, p 237-244
 11. C. **Rocchiccioli-Deltcheff**, Practice of the Statistical Methods to the Analysis, *Les Techniques de l'Ingénieur*, Paris, M7, p 5000.1-5000.14 (in French)
 12. M. **Vigier**, Practice of Experimental Designs: The Taguchi Methodology, Les Editions d'Organisation, Paris, 1988 (in French)
 13. L. **Regnier**, M. Beguere, and N. Coue, "Taguchi Methodology: The Renewal of the Experimental Designs. Parts I and II," Reports RI 89-302 and RI 90-320, **IRSID**, Saint Germain. France. 1989 (in French)
 14. NIH Image 1.49 Reference Manual, NIH Image is a public domain image processing and analysis program.
 15. L. Devore, Probability and Statistics for Engineering and the Sciences, 3rd ed., Brooks-Cole Publishing, Pacific Grove, CA, 1991
 16. B. **Bergman**, On the Estimation of the Weibull Modulus, *J. Mater. Sci. Lett.*, Vol 3, 1984, p 689-692
 17. W. Weibull, A Statistical Distribution Function of Wide Applicability, *J. Appl. Mech.*, Vol 18, 1951, p 293-297
 18. P.R. Bevington, Estimates of Mean and Errors, chap. 5, Data Reduction and Error Analysis for the Physical Sciences, **McGraw-Hill**, 1985, p 66-133
 19. R.B. Abernethy, J.E. Breneman, C.H. Medlin, and G.L. **Reinman**, Weibull Analysis Handbook, Report **AFWAL-TR-83-2079**, Air Force Wright Aeronautical Laboratories, Nov 1983
 20. J.F. Lawless, Statistical Models and Methods for Lifetime Data, John Wiley & Sons, 1982, p 141-202
 21. C.C. Berndt, J. Ilavsky, and J. **Karthikeyan**, Microhardness-Lifetime Correlations for Plasma Sprayed Thermal Barrier Coatings. Thermal Spray: International Advances in Coatings Technology, C.C. Berndt, Ed., ASM International, 1992. p 941-946
 22. J.M. Houben, "Relation of the Adhesion of Plasma Sprayed Coatings to the Process Parameters Size, Velocity and Heat Content of the Spray Particles," **Ph.D.** thesis, Polytechnic University of **Eindhoven**, **Eindhoven**, The Netherlands. Nov 1988
 23. A. Roux, "Contribution to the Study of the Particles/Plasma Energy Transfer in the Case of Radio-Frequency and d.c. Plasmas," **Ph.D.** thesis, **Université de Compiègne-Sévenans, Sévenans**, France, June 1991 (in French)
 24. P. Fauchais, A. Vardelle, M. Vardelle, F. Monerie, A. Denoirjean, and A. Grimaud, Influence of the Thermo-Kinetic Phenomena during Particulate Impact on the Properties of Ceramic Coatings, Thermal Spray Coatings: Properties, Processes and Applications, T.F. **Bernecki**, Ed., ASM International, 1992, p 205-216
 25. H. Liu, E.J. **Lavernia**, and R.H. **Rangel**, Numerical Simulation of Impingement of Molten Ti, Ni, and W Droplets on a Flat Substrate, *J. Therm. Spray Technol.*, Vol 2 (No. 4). 1993, p 369-378
 26. M. **Kitaura**, J. Yao, J. Senda, and H. **Fujimoto**, in Proc. 13th Japanese **Conf.** Atomization of Liquids, The Japan Institute of Metals (Tokyo), 1984, p 221-226

JOURNAL OF

THERMAL SPRAY

TECHNOLOGY

INSIDE:

Modeling the
Deposition
Process

Modeling of Particles
Impacting on a
Rigid Substrate

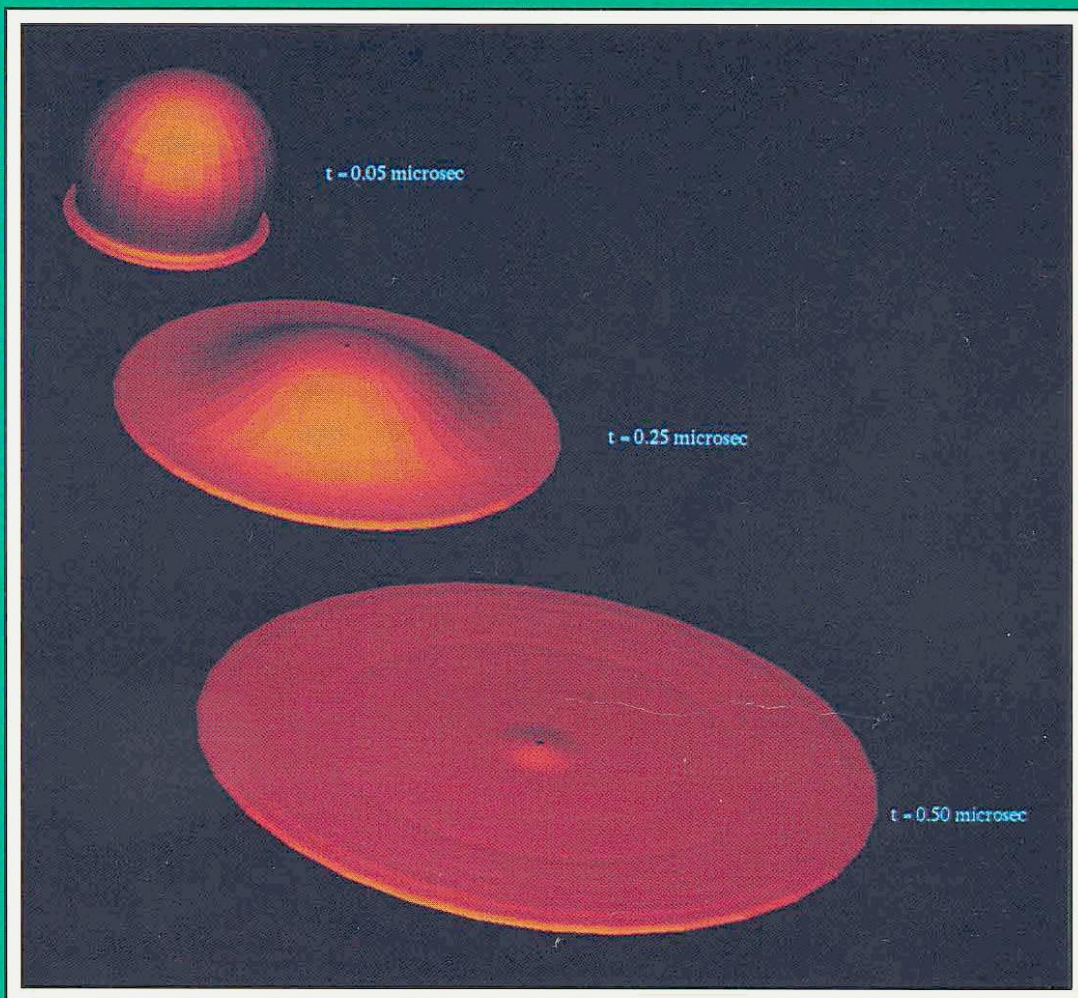
Quenching Stress

Influence of Particle
Parameters at Impact
on Splat Formation
and Solidification

Splat Morphology

RF and DC Plasma
Spraying

and much more!



Christopher C. Berndt, Editor in Chief
Pierre Fauchais, Guest Editor